ISSN No. 0976-5697

Volume 2, No. 3, May-June 2011

International Journal of Advanced Research in Computer Science

RESEARCH PAPER

Available Online at www.ijarcs.info

Quantitative Analysis for the Identification of Brain Tumor in CT and MRI Medical Images

S Rajkumar*
Assistant Professor
School of Computer Science and Engineering
VIT University, Vellore
rajkumars@vit.ac.in

S Kavitha
Assistant Professor
Department of Computer Science and Engineering
SSN College of Engineering,
Chennai,IndiaS
kavithas@ssn.edu.in

Abstract: The fusion in medical images is necessary, to derive the require information from multimodality medical images for diseases diagnosis. This paper describes a multimodality medical image fusion system using different fusion techniques and the resultant is analysed with quantitative measures. Initially, the registered images from two different modalities such as CT (anatomical information) and MRI - T2, FLAIR (pathological information) are considered as input, since the diagnosis requires anatomical and pathological information. Then the fusion techniques namely Redundancy Discrete Wavelet Transform (RDWT), Contourlet Transform and Multiple-Pulse Coupled Neural Network (M-PCNN) are applied. Further the fused image is analyzed with four types of quantitative metrics such as Standard Deviation (SD), Entropy (EN), Overall Cross Entropy (OCE), and Power Signal to Noise Ratio (PSNR) for performance evaluation. From the experimental results we observed that RDWT method provides better information (quality) using EN metric and the Contourlet Transform gives the difference in source to the fused image using OCE metric and M-PCNN method offer the more contrast information using PSNR metric and also the fused image obtained from the proposed fusion techniques has more information than the source images are proved through all metrics.

Keywords: Medical image fusion; Multimodality images; Redundancy Discrete Wavelet Transform; Contourlet Transform; Multiple-Pluse Coupled Neural Network; Quantitative Metrics

I. INTRODUCTION

In the field of Medical imaging, the radiologists require high resolution medical images with all information such as region, tissue and visualization for disease diagnostics. This constraint is not resolved with single modality medical images since: the X-ray Computed Tomography (CT) is more popular with recognizing bone structure; the soft tissue information's are more visible in Magnetic Resonance Image (MRI); Positive Electron Tomography (PET) provides better clear information in blood flow and so on. In reality for efficient disease diagnosis, complementary information from multiple modalities is required. In this corner only the fusion techniques has attracted more researchers in this domain to assist the physicians in fusing and retrieving information from different modalities such as CT, MRI, PET, SPECT fMRI and so on [12].

In the research of fusion techniques, many approaches are proposed and implemented. Some of these methods are available in Fusion Tool of Matlab5.0 namely are Filter-Subtraction-Decimate Pyramid (FSD), Gradient Pyramid, Laplacian Pyramid [9], Discrete Wavelet Transform Pyramid (DWT), Shift Invariant Discrete Wavelet Transform Pyramid (SIDWT) [8], Principle Component Analysis [2], Morphological Pyramid, Ratio Pyramid, Contrast Pyramid, and so on [1]. In all the above methods each approach has its own limitation in fusion process. For example, Contrast Pyramid method loses too much information from the source images; Ratio Pyramid method produces lots of false information that does not exist in the source images; and Morphological Pyramid method creates many false edges. In a word, these methods cannot deal with various types of medical images .

The majority of fusion techniques are based on wavelet transformation [3]. But, the DWT in medical image fusion is resulting with shift variant and additive noise in fused image. These issues can be resolved using Redundancy Discrete Wavelet Transform (RDWT) and Contourlet Transform.

RDWT preserves the exact edge and spectral information without much of spatial distortion [11]. It also provides shift invariant to overcome the shift variant problem of DWT. In this method, the low pass and high pass sub bands of the input images are fused using average method and entropy method respectively.

The region based Contourlet Transform brings local brightness, multiresolution, localization, directionality and anisotropy, etc. on the fused image [6]. This method is implemented in two stages namely transformation and sub band decomposition. In the transformation stage, double filter bank is applied and in the decomposition stage, local energy of each sub band is calculated and then fusion rule (Average mode or Selection mode) is applied. This is a part of a multi-dimensional signal processing theory called as Multiscale Geometric Analysis (MGA) Tools.

M-PCNN is a biologically inspired neural network model fusion technique. It is mainly designed to avoid the PCNN problem i.e. one PCNN cannot finish the whole process of image fusion.

The M-PCNN approach consists of three parts: dendritic tree, information fusion, and pulse generator. The role of the dendritic tree is to receive two kinds of inputs. One is from the external stimulus and another is from the surrounding neurons. Information fusion is the place where all data is fused. The role of the pulse generator is to generate output pulse

The performance of the fusion techniques are evaluated based on different quantitative metrics such as SD, EN, OCE, PSNR.

The remaining sections of this paper are organized as follows. In Section II, the system design is briefly reviewed; section-III describes experimental results and evaluates the performance of the proposed methods based on the quantitative metrics. Discussion and future work are summarized at the end.

II. SYSTEM DESIGN

In this novel system initially the two different types of modality images CT (anatomical) and MRI (pathological) are given as input. Then the fusion techniques are applied to the registered images to find a more informative fused image. The fused image is validated using quantitative measures. The system design is shown in Fig. 1.

A. Dataset

The dataset (images) are collected from Indian Scan Center, Madurai, Tamil Nadu, India. The images are acquired from the organ (Brain) at different modality such as CT and MRI (MR-T2 and MR-FLAIR). Each set of image is taken from the same patient at different modality.

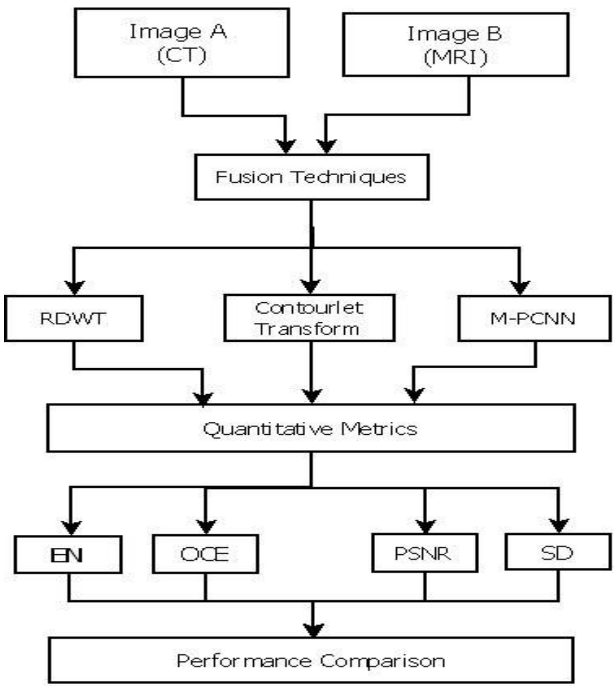

Figure 1. An overall view of system design

B. Redundancy Discrete Wavelet Transform

RDWT fusion technique can be effectively performed for registered images of different modality (CT and MRI) or images captured at different time instances (T1, T2 and FLAIR) [6].

Let A_1 and B_1 be the registered images of different modalities (CT and T2) or (CT and FLAIR). Three levels of RDWT decomposition is done using Daubechies filters on both the images to obtain an approximation wavelet bands shown in Fig. 2 [4].

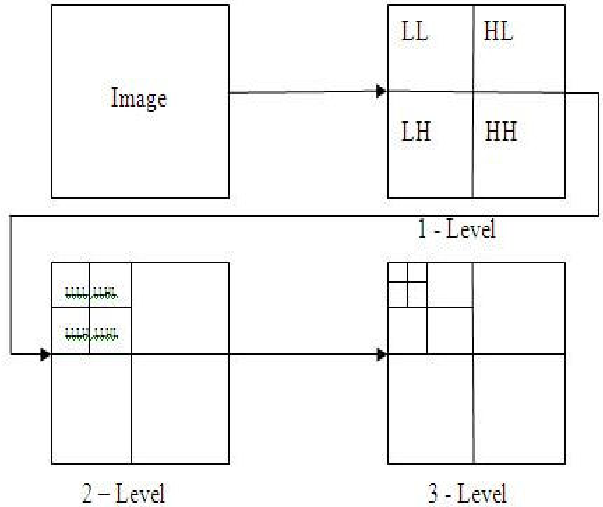

Figure 2. Three levels of decomposition

In the first stage I_1 image is decomposed into I_1^a, I_1^v, I_1^d, and I_1^h be the RDWT subbands and also I_2^a, I_2^v, I_2^d, and I_2^h be the corresponding RDWT subbands from I_2 image. To extract the features from both the images, coefficients from approximation band of I_1 and I_2 are averaged;

$$I_F^a = \mathrm{mean}(I_1^a, I_2^a) \tag{1}$$

where I_F^a is the approximation band of the fused image.

In the next stage each subband namely LH, HL, HH is divided into blocks of size 3 * 3 and the entropy of each block is calculated, as in (2).

$$e_i^{jk} = \ln\sqrt{(\mu_i^{jk} - \sum_{x,y=1}^{3,3} I_i^{jk}(x,y)/\sigma_i^{jk})^2/m^2} \tag{2}$$

where j (= v, d, h) denotes the subbands, m = 3 (size of each block), k represents the block number, and i (= 1,2) is used to differentiate the two multimodal images I_1 and I_2. μ_i^{jk} and σ_i^{jk} are the mean and standard deviation of the RDWT coefficients. Using the entropy values, the detail subbands for the fused image I_F^v I_F^v, I_F^d, and I_F^h are generated, as in (3). The derive a fused image block I_F^{jk}, RDWT coefficients from I_1 is selected if the entropy value of the specific block of I_1 image is greater than the specific block of I_2 image, otherwise I_2^{jk} is selected.

$$I_F^{jk} = \begin{cases} I_1^{jk}, & \text{if } (e_1^{jk)} > e_2^{jk}) \\ I_2^{jk}, & \text{otherwise} \end{cases} \tag{3}$$

Finally, IRDWT is applied on all the four fused subbands to generate the resultant fused medical image I_F.

$$I_F = \mathrm{IRDWT}(I_F^a, I_F^v, I_F^d, I_F^h) \tag{4}$$

C. Contourlet Transform

Contourlet transform brings smoothness in a fused image with any two different modalities of images [6]. This region based transformation is implemented in two stages. In the first stage double filter bank scheme is applied for transformation and in the next stage decomposition is done with fusion rules. Finally the fused image is retrieved using reconstruction procedure.

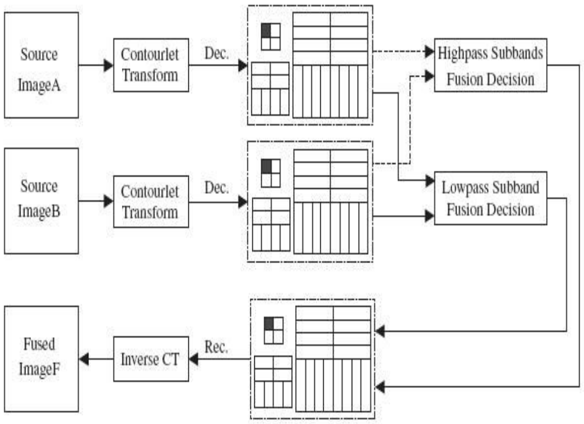

Figure 3. Block diagram of the contourlet based image fusion

The flow graph of the proposed image fusion algorithm is shown in Fig. 3. Here image A and B denotes the input source images CT and MRI respectively. F is the final fused outcome after inverse contourlet transform.

1) Transformation Stage

In this stage a double filter bank scheme is utilized efficiently for subband decomposition using Laplacian Pyramid (LP) and Directional Filter Bank (DFB). Laplacian pyramid filter is used to capture the edge point. Directional Filter Bank is used to link the discontinuities point in linear structures.

In Laplacian Pyramid method each input image is decomposed into a subband of low frequency of original image and a bandpass high frequency subbands [5]. The same process is repeated for low frequency subband for the specified contourlet decomposition level. The Laplacian Pyramid decomposition process is shown in Fig. 4. The input image is applied to a LP filter *H* and then down sampled to derive a coarse approximation *a* (Lowpass Subband). Then the image is up sampled and passed through a synthesis filter *G*. The resultant highpass subbands are derived from subtracting the output of the synthesis filter with the input image.

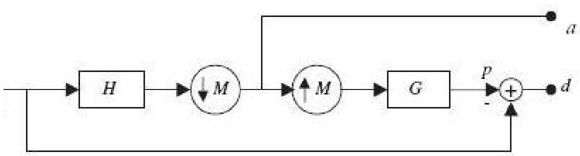

Figure 4. Construction of LP

In addition Directional Filter Bank [7] is used for highpass subbands using quincunx filter to form a tree structure image. The Directional Filter Bank diagram is shown in Fig. 5. For each of the highpass subband, down sampling and up sampling is done and the resultants are passed to synthesis filter. The output of synthesis filter is combined.

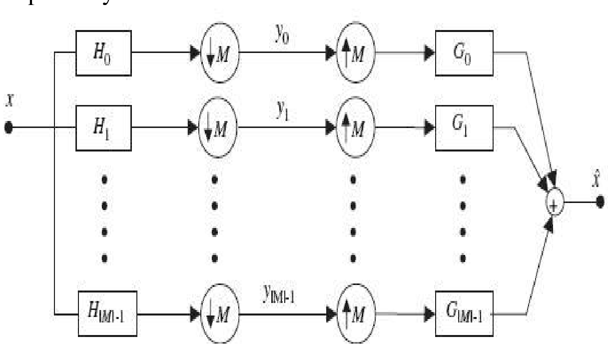

Figure 5. Construction of DFB

2) Decomposition Stage

The decomposed subbands of transformation stage are combined using Lowpass and Highpass Fusion rules.

a) Lowpass subband fusion: The coefficients in the coarsest scale subband a represents the approximation component of the source image. Here the local energy contourlet domain is developed as the measurement, then the selection and averaging modes are used to compute the final coefficients [5].

The local energy E(x,y) is calculated centering the current coefficient in the approximate subband a, which is

$$E(x,y)=\sum_m \sum_n a_j(x+m,y+n)^2 W_L(m,n) \tag{5}$$

where (x,y) denotes the current contourlet coefficient, $W_L(m,n)$ is a template of size 3*3

$$W_L = 1/9 * \begin{matrix} 1 & 1 & 1 \\ 1 & 1 & 1 \\ 1 & 1 & 1 \end{matrix} \tag{6}$$

Then the salience factor is calculated to determine whether the selection mode and averaging mode to be used in the fusion process.

$$M_j^{AB}(x,y) = 2\sum_m \sum_n a_j^A(x+m,y+n)a_j^B(x+m,y+n)/E^A(x,y)+E^B(x,y) \tag{7}$$

where $a_j^x(x,y)$; x=A,B denotes the lowpass contourlet coefficients of the source image A or B *and* $M_j^{AB}(x,y)$ is the salience factor.

Salience factor reflects the similarity of the lowpass subbands of the two source images. Then this value is compared to a predefined threshold T_L ($T_{L=}1$). If $M_j^{AB}(x,y) > T_L$, averaging mode is selected for fusion in (8).

$$a_j^F(x,y) = \alpha_A .\ a_j^A(x,y) + \alpha_B .\ a_j^B(x,y) \tag{8}$$

where $a_j^F(x,y)$ is fused result at position (x,y). The α_A and α_B are selected based on the condition specified, as in (9).

$$\alpha_{A} = \begin{cases} \alpha_{min} & \text{for } E^A(x,y) < E^B(x,y) \\ \alpha_{max} & \text{for } E^A(x,y) >= E^B(x,y) \end{cases} \tag{9}$$

where $\alpha_B = 1 - \alpha_A$, α_{min} € (0,1) $\alpha_{min} + \alpha_{max} = 1$

The selection mode is chosen for the condition $M_j^{AB}(x,y) <= T_L$, with the fusion rules denoted in (10).

$$a_j^F(x,y) = \begin{cases} a_j^A(x,y) & \text{for } E^A(x,y) >= E^B(x,y) \\ a_j^B(x,y) & \text{for } E^A(x,y) < E^B(x,y) \end{cases} \tag{10}$$

b) Highpass subband fusion: The coefficients with larger absolute values in the high frequency subbands dj,k are fused using average method is defined as follows

$$E^F_{j,k}(x,y) = d^A_{j,k}(x,y) + d^B_{j,k}(x,y) \tag{11}$$

where $E^F_{j,k}(x,y)$ is the local energy, $d^X_{j,k}(x,y)$ is the high frequency coefficient

c) Reconstruction of fusion image: The fused image is constructed from $a_j^F(x,y)$ and $E^F_{j,k}(x,y)$ using inverse contourlet decomposition method.

D. *Multiple-Pulse Coupled Neural Network*

The M-PCNN model consists of three parts: dendritictree, information fusion, and pulse generator., as shown in fig. 6.

The role of the dendritic tree is to receive two kinds of inputs. Based on the received input, it is divided into the external stimulus and the surrounding neurons. Information fusion is the place where all data is fused. The role of the pulse generator is to generate output pulse

In our model can adjust the number of external input channels according to the needs. Here, there are m input channels. Generally, m>1. so both stimuli can be input into the model at the same time[13].

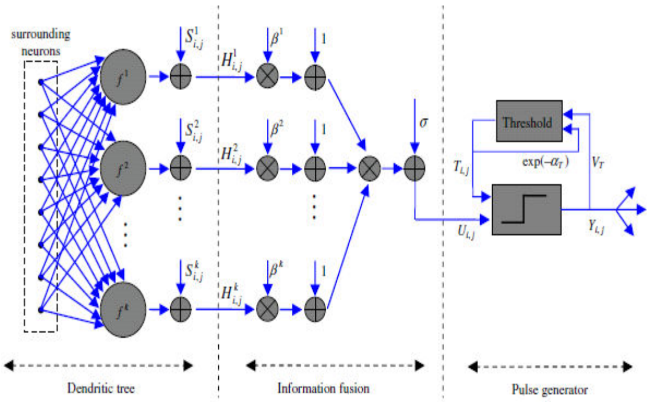

Figure 6. Block Diagram of M-PCNN

Following things are mathematically describe its model.

$$H_{i,j}^{k}[n] = f^{k}(Y[n-1]) + S_{i,j}^{k} \qquad (12)$$

$$U_{i,j}[n] = \pi_{k=2}^{K} (1 + \beta^{k} H_{i,j}^{k}[n]) + \sigma \qquad (13)$$

$$Y_{i,j}[n] = 1,\ U_{i,j}[n] > T_{i,j}[n-1] \qquad (14)$$

$$T_{i,j}[n] = \exp(-\alpha_T) T_{i,j}[n-1] + V_T Y_{i,j}[n] \qquad (15)$$

where H^K refers to the channel of the k^{th} external input, S^k, k = 2,3,....,K and $f^k(.)$ is the feed function, which shows the influence of surrounding neuron on the current neuron. B^k refers to the weighting factor of the k^{th} channel; usually, $0<\beta^k<1$. The value of β^k can be increased to stress its importance of the k^{th} channel. If all the inputs have parallel importance, the factors usually will be set to the same constant. σ is the level factor to adjust the average level of internal activity. $U_{i,I}[n]$ is the internal state of the neuron. $Y_{i,j}[n]$ depends on the internal state and threshold. $T_{i,j}[n]$ is the dynamic threshold of the neuron. V_T and α_T are normalized constant and time constant, respectively.

E. *Quantitative Analysis on Fused Image*

The quantitative measurement is done on the fused images using some objective and subjective quality measures. It helps better in assessing the information of images. This section explains the quantitative metrics used in the analysis of this system.

1) Standard Deviation (SD): The standard deviation defines the contrast information of an image. The image with more contrast has high value of standard deviation where as low value for minimum contrast images [10]

$$\sigma = \sqrt{1/N \sum_{i=1}^{N} (xi - x)^2} \qquad (16)$$

where x is defined as a summation

$$x = 1/N \sum_{i=1}^{N} xi = x_1 + x_2 + \ldots + x_N/N \qquad (17)$$

2) Entropy (EN): Entropy can effectively reflect the amount of information in certain image. The larger value indicates, the better fusion result is obtained [5]

$$EN = -\sum_{i=0}^{L-1} P_F(i) \log_2 P_F(i) \qquad (18)$$

where P_F is the normalized histogram of the fused image to be evaluated, *L* is the maximum gray level for a pixel in the image. In our tests, *L* is set to 255.

3) Overall Cross Entropy (OCE): The overall cross entropy is used to measure the difference between the two source images and the fused image. The minimum value corresponds to good fusion result is obtained [5].

$$OCE(f_A, f_B; F) = CE(f_A; F) + CE(f_B; F)/2 \qquad (19)$$

where f_A,f_B are the source images, F is the fused result, $CE(f_A;F)$ $CE(f_B;F)$ are the cross entropy of the source image f_A (f_B) with the fused image F respectively. The cross entropy is defined as

$$CF(G,F) = \sum_{i=0}^{L-1} P_G(i) \log_2 |P_G(i)/P_F(i)| \qquad (20)$$

G=A or B

4) Power Signal to Noise Ratio (PSNR): PSNR of an image is usually defined as the ratio of the mean pixel value to the standard deviation of the pixel values [10].

$$PSNR = Mean/Standard\ Deviation \qquad (21)$$

It is more or less same as standard deviation.

III. EXPERIMENTAL RESULTS AND PERFORMANCE EVALUATION

The experimental result of the fusion techniques are analyzed with six brain images taken from CT and MRI (T2 and FLAIR). Each CT image is combined with either T2 or FLAIR and considered as one set for fusion. Thus in turn totally derives twelve combinations as input dataset. All images have the same size of 256 * 256 pixels, with 256-level gray scale. Some of the sample images are shown in Fig. 7-8.

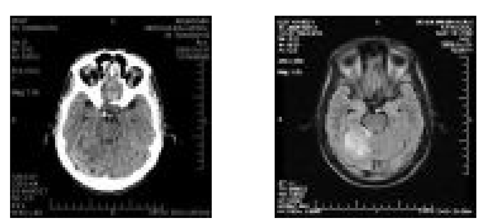

CT MRI-T2

Figure 7. Dataset4-CT and MRI-T2

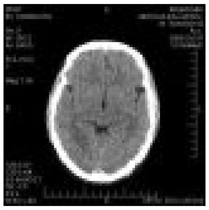
CT

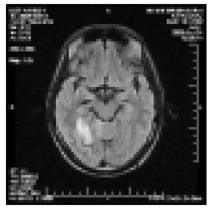
MRI-FLAIR

Figure 8. Dataset10-CT and MRI-FLAIR

In our experiment, RDWT decomposition is done for three different levels and a 2-level of decomposition is done for Contourlet Transformation and also the input images of each set are fused using M-PCNN. The resultant image of each technique is shown in Fig. 9.

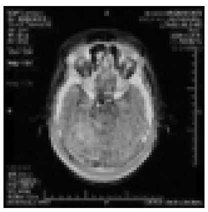
RDWT – Level 1

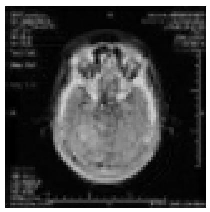
RDWT – Level 2

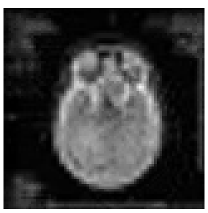
RDWT – Level 3

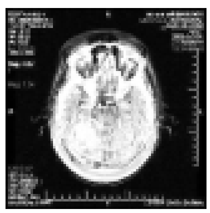
Contourlet Transform – Level 2

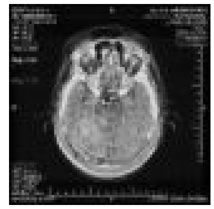
M-PCNN

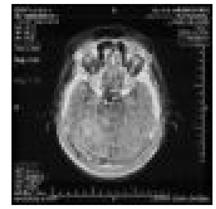
M-PCNN

Figure 9. Fused images of Dataset 4

The fused image obtained from each technique is analyzed with quantitative metrics discussed in the section II. The results of all the techniques used to analyze the fused image with the metrics are shown in the TABLE I-II and representation of the graph in Fig 10-17.

The graph in Fig 10-13, x axis represents the data set (1-6) and y axis represent the corresponding values derived from the specific metric for each of the proposed Method.

The graph in Fig 14-17 x axis represent with the data set (7-8) and y axis represent the corresponding values derived from the specific metric for each of the proposed method

TABLE I. COMPARISON OF IMAGE FUSION ALGORITHM FOR CT AND MRI-T2 TIME

Metrics	Algorithm	Image set 1	Image set 2	Image set 3	Image set 4	Image set 5	Image set 6
EN	**RDWT-level 1**	6.6690	6.6574	6.5769	6.6674	6.7159	6.6363
	RDWT-level 2	6.7636	6.7414	6.6635	6.7522	6.7944	6.7908
	RDWT-level 3	6.8407	6.7869	6.7195	6.8123	6.8533	6.6668
	Contourlet-level 2	6.3934	6.1640	6.3263	6.3267	6.3367	6.3542
	M-PCNN	6.6730	6.7513	6.6612	6.7225	6.7450	6.6336
OCE	**RDWT-level 1**	1.0705	3.7607	3.7873	2.7278	2.9605	2.2524
	RDWT-level 2	1.7954	3.2571	3.1154	3.7660	3.7405	3.0920
	RDWT-level 3	1.3620	3.0505	2.7211	3.3382	3.3529	3.3516
	Contourlet-level 2	-1.3532	0.8446	0.1941	0.4176	0.4479	-0.1390
	M-PCNN	2.1718	3.6402	4.5258	4.6119	4.9841	4.4590
PSNR	**RDWT-level 1**	0.4576	0.4325	0.4255	0.4384	0.4540	0.4507
	RDWT-level 2	0.4694	0.4405	0.4313	0.4467	0.4624	0.4335
	RDWT-level 3	0.4441	0.4048	0.4065	0.4236	0.4362	0.4390
	Contourlet-level 2	0.4146	0.3752	0.3929	0.3815	0.3947	0.3982
	M-PCNN	0.5185	0.5221	0.5158	0.5130	0.5233	0.5114
SD	**RDWT-level 1**	16.779	17.756	18.047	17.517	16.912	17.036
	RDWT-level 2	16.360	17.433	17.803	17.189	16.606	17.713
	RDWT-level 3	17.290	18.969	18.889	18.128	17.604	17.491
	Contourlet-level 2	18.520	20.465	19.545	20.128	19.456	19.284
	M-PCNN	14.810	14.709	14.887	14.969	14.674	15.016

TABLE II. COMPARISON OF IMAGE FUSION ALGORITHM FOR CT AND MRI-FLAIRTIME

Metrics	Algorithm	Image set 7	Image set 8	Image set 9	Image set 10	Image set 11	Image set 12
EN	**RDWT-level 1**	6.6090	6.6574	6.5769	6.6674	6.7159	6.6363
	RDWT-level 2	6.7128	6.7414	6.6635	6.7522	6.7944	6.7908
	RDWT-level 3	6.7888	6.7869	6.7195	6.8123	6.8533	6.6668
	Contourlet-level 2	6.2620	6.1640	6.3263	6.3267	6.3367	6.3542
	M-PCNN	6.6223	6.7513	6.6612	6.7225	6.7450	6.6336
OCE	**RDWT-level 1**	3.9805	3.7607	3.7873	2.7278	2.9605	2.2524
	RDWT-level 2	3.6913	3.2571	3.1154	3.7660	3.7405	3.0920
	RDWT-level 3	3.6280	3.0505	2.7211	3.3382	3.3529	3.3516

	Contourlet-level 2	1.1077	0.8446	0.1941	0.4176	0.4479	-0.1390
	M-PCNN	3.8376	3.6402	4.5258	4.6119	4.9841	4.4590
PSNR	**RDWT-level 1**	0.4171	0.4325	0.4255	0.4384	0.4540	0.4507
	RDWT-level 2	0.4373	0.4405	0.4313	0.4467	0.4624	0.4335
	RDWT-level 3	0.4179	0.4048	0.4065	0.4236	0.4362	0.4390
	Contourlet-level 2	0.3667	0.3752	0.3929	0.3815	0.3947	0.3982
	M-PCNN	0.4813	0.5221	0.5158	0.5130	0.5233	0.5114
SD	**RDWT-level 1**	18.408	17.756	18.047	17.517	16.912	17.036
	RDWT-level 2	17.558	17.433	17.803	17.189	16.606	17.713
	RDWT-level 3	1.8376	18.969	18.889	18.128	17.604	17.491
	Contourlet-level 2	20.941	20.465	19.545	20.128	19.456	19.284
	M-PCNN	15.956	14.709	14.887	14.969	14.674	15.016

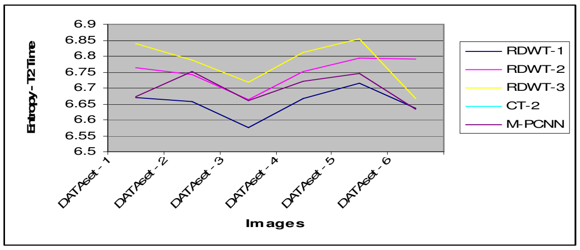

Figure 10: Graph – 1 Entropy Calculation

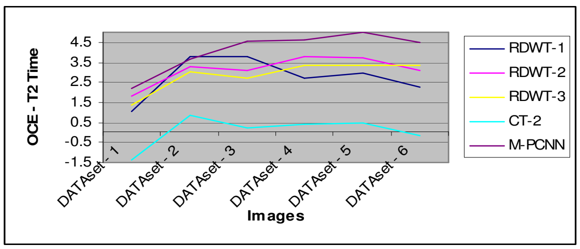

Figure 11: Graph – 2 Overall Cross Entropy Calculation

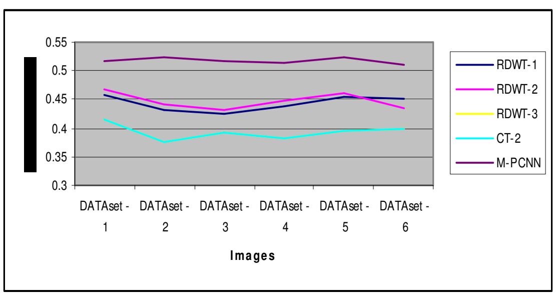

Figure 13: Graph – 3 Power Signal to Noise Ratio Calculation

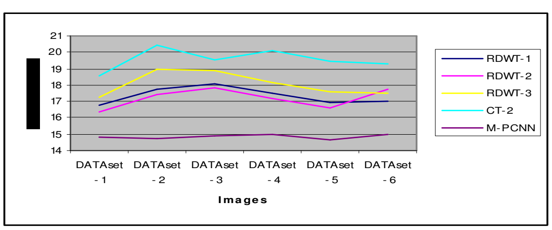

Figure 14: Graph – 4 Standard Deviation Calculation

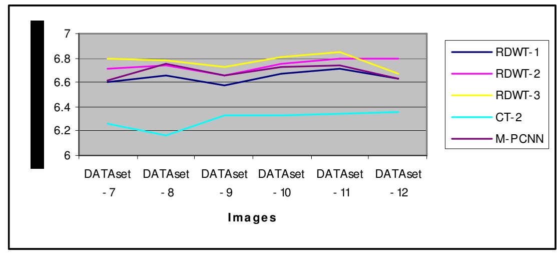

Figure 15: Graph -5 Entropy Calculation

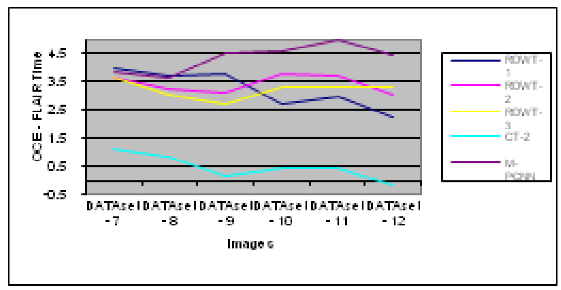

Figure 16: Graph -6 Overall Cross Entropy Calculation

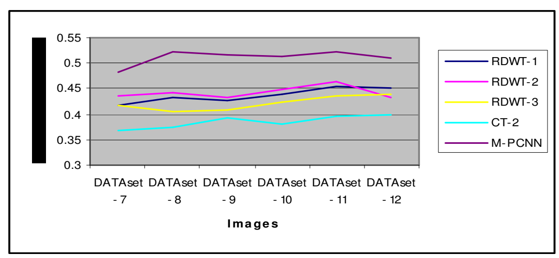

Figure 17: Graph – 7 Power Signal to Noise Ratio Calculation

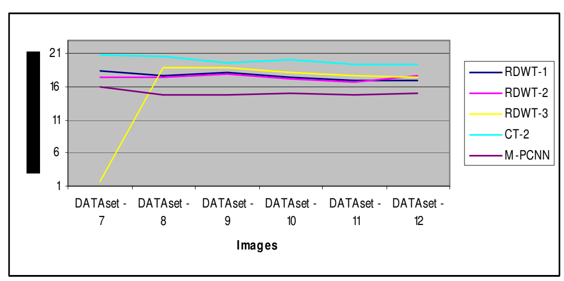

Figure 18: Graph – 8 Standard Deviation Calculation

DISCUSSION AND FUTURE WORK

In this paper, three different fusion techniques with quantitative metrics are analyzed with brain images acquired from CT and MRI at two different times (T2 & FLAIR)for twelve sets . From the above TABLE I-II and the graphs (10-17), It concludes that RDWT technique provides better information using EN metric, and the Contourlet Transform method gives the difference in source to the fused image using OCE metric and M-PCNN method offer the more contrast information using PSNR metric and the same is justified with the visualization of the fused image also. The PSNR metric value ensures the contrast information of the fused image. The fusion techniques lead to many computational merits in reality namely reduction in storage space/cost, efficiency in retrieval of data and data replication. All the computational merits are assumed to be avoided.

In Future, This can be extended to incorporate learning techniques and various medical modality images (fMRI, PET, SPECT etc) for fusion to assist the physicians of the real world in disease diagnosis.

V.ACKNOWLEDGMENT

The authors would like to thank Indian Scan Center, zMadurai, Tamil Nadu, India, for providing the Brain images of same patient at different modality.

VI. REFERENCES

[1] Firooz Sadjadi, “Comparative Image Fusion Analysis”, IEEE Coputer Society Conference on Computer Vision and Pattern Recognition, vol. 3, June 2005.

[2] Huaixin Chen, "A Multiresolution Image Fusion Based on Principle Component Analysis", Fourth International Conference on Image and Graphics, pp. 737-741,August 2007.

[3] J.Fowler, “The Redundant Discrete Wavelet Transform and Additive Noise”, IEEE Signal Proessing Letters, vol. 12, pp. 629-632, September 2005.

[4] Ligia Chiorean, Mircea-Florin Vaida, “Medical Image Fusion Based on Discrete Wavelet Transform using Java Technology, 31st International Conference on Information Technology Interfaces, pp. 22-25, June 2009.

[5] L.Yang, B.L.Guo, W.Ni, “ Multimodality Medical Image Fusion Based on Multiscale Geometric Analysis of Contourlet Transform”, Elsevier Science Publishers, vol. 72, pp. 203-211, December 2008.

[6] L. Yang, B.L.Guo, W.Ni, “Multifocus Image Fusion Algorithm Based on Contourlet Decomposition and Region Statistics” , Fourth International Conference on Image and Graphics, pp. 707-712, Septemper 2007.

[7] Minh N. Do, “The Contourlet Transform: An Efficient Directional Multiresolution Image Representation”, IEEE Transaction on Image Processing, Vol. 14,pp. 2091-2106, November 2005

[8] Oliver Rockinger, "Image Sequence Fusion Using a Shift-Invariant Wavelet Transform", International Conference on Image Processing, vol. 3, pp. 288, October 1997.

[9] Peter J.Burt, Edward H.Adelson, "The Laplacian Pyramid as a Compact Image Code", IEEE Transactions on Communications, vol. 31, pp. 532-540, April 1983.

[10] R.Maruthi R.M.Suresh, “Metrics for Measuring the Quality of Fused Images”, International Conference on Computational Intelligence and Multimedia Applications, pp. 153-158, December 2007.

[11] Richa Singh, Mayank Vatsa, “Multimodal Medical Image Fusion using Redundant DiscreteWavelet Transform”, In proceedings of Seventh International Conference on Advances in Pattern Recognition, pp. 232-235, February 2009.

[12] S.Rajkumar, S.Kavitha, “ Redundancy Discrete Wavelet Transform and Contourlet Transform for Multimodality Medical Image Fusion with Quantitative Analysis”, 3rd International Conference on Emerging Trends in Engineering and Technology, November 2010.

[13] Zhaobin Wang, Yide Ma, “ Medical image fusion using m-PCNN”, Information Fusion, vol 9, pp. 176-185, April 2007.